Study of Summer Lake, OR BB3-I Core via Biogeochemical Molecular and Isotopic Analysis for Paleoclimate Reconstruction

By

Dawn A. Fetzer, M.S.

A Thesis Submitted to the Department of Geological Sciences, California State University Bakersfield in Partial Fulfillment for the Degree of Masters of Geology.

Spring 2016

Study of Summer Lake, OR BB3-I Core via Biogeochemical Molecular and Isotopic Analysis for Paleoclimate Reconstruction

By

Dawn A. Fetzer

This thesis or project has been accepted on behalf of the Department of Geology by their supervisory committee:

Robert Negrini

Committee Chair

Roy LaFever

Anna Jacobsen

Acknowledgements

My deepest gratitude is to my advisor Dr. Rob Negrini. I want to thank Rob for advising me to get my degree in geology in the beginning and staying with me until the very end. I have been very fortunate to have been taken on as his last research student prior to retirement. I also want to thank Rob for believing in me to finish this manuscript in time when he did not have to. When writing my manuscript Rob helped me to sort out the technical details of my work; I am grateful to him for holding me to a high research standard and enforcing strict validations for each result. Rob not only offered me a great topic but also an opportunity for me to work with two great advisors of different disciplines.

I am immensely grateful to Dr. Roy Lafever. Roy has always been available to listen and provide advice to me since my time as an undergraduate student in Chemistry. Roy has been one of the best professors I have ever had and a person that I look up to. I want to thank Roy for pushing me, believing in me, providing me with support, giving me advice and his willingness to meet at any time in order to meet this deadline. Roy has been instrumental in the research necessary for this thesis and has made available his support in a number of ways.

I am forever thankful to my co-workers at CRC, specifically Vaughn Thompson. Thank you for your encouragement, support and continuous optimism. Vaughn's insightful comments and constructive criticisms were thought-provoking and helped me focus my ideas when writing my manuscript. Thank you for believing in me and supporting me in both my career and education.

Most importantly, the love and patience of my family has helped keep me sane while continuing my education. Their support helped get me through the long journey of a double major in Chemistry and Geology as well as the completion of my MS in Geology. I appreciate their generosity and understanding over these years.

A special thanks to Dr. Anna Jacobson for being a co-advisor on my thesis, a co-author on the associated manuscript, and providing advice from a biologist's standpoint.

Thank you to Florida International University Stable Isotope Lab for providing me with isotope results.

Abstract

The purpose of this study is to test models of millennial-scale climate response to hemispheric-scale drivers during the late Pleistocene in northwestern North America. Towards this end, a 12.5-10.5 mbgs section of the BB3-I core, spanning 38-35 ka in age and taken from Summer Lake Basin, Oregon, USA, was investigated using lipid molecular stratigraphy and compound specific carbon isotope analysis. Previous climate proxy studies on this core segment, including those based on C_{org}/N, ostracode taxonomy, palynology, and environmental magnetism, divided the core segment into four intervals of alternating warmer/wetter and cooler/drier climate corresponding to Dansgaard-Oeschger (D-O) Interstadials #8 and #7 and the successive stadials.

Carbon isotope ratios ranged from -24.5 to -42.4 ‰ indicating that as expected, all plants represented by the leaf waxes followed the C_3 photosynthetic pathway. ACL_{25-33} (Average Chain Length) and CPI_{23-35} (Carbon Preference Index) values in the sediment samples associated with the D-O interstadials were higher (30.31 - 29.61) than the ACL values for the stadials, particularly the one that followed IS#7, indicating the dominance of terrestrial-sourced vegetation during interstadials and aquatic vegetation during stadials. Similarly, P_{aq} values were lower during interstadials and vice-versa indicating an increased terrestrial component of organic matter rather than organics of strictly lacustrine origin. Furthermore, a preference for terrestrial origin in interstadial samples was found in the odd carbon-numbered, long-chain *n*-alkanes with the younger stadial sample identified to be exclusively aquatic/lacustrine. These results support the teleconnection hypothesis of climate response to late Pleistocene millennial-scale climate change in the North American Great

Basin wherein warmer temperatures in the North Atlantic drive wetter, warmer Great Basin climates and vice-versa.

Keywords: *N*-alkanes, Paleoclimate, Summer Lake, Geochemistry, Leaf-wax *N*-alkanes, Paleoenvironment

Table of Contents

List of Figures

List of Tables

List of Equations

1. Introduction

The effect of millennial-scale climate changes during the past glaciation on northern hemisphere landscapes is poorly understood. The present study endeavors to increase this understanding using the methods of molecular geochemistry. The sediments of Summer Lake were chosen for this study due to favorable lipid preservation and accumulation conditions in this lake bed and due to extensive previous studies from which a testable hypothesis emerged.

Most lake sediments contain only a small amount of organic matter but through extraction and quantification, these hydrocarbons can be used to determine various organic material sources. Plants, algae, and bacteria contain varying concentrations of normal alkanes (*n*-alkanes) provided by leaf waxes in vascular plants and cell membranes in algae. *N*-alkanes are lipid extracts in the form of hydrocarbon chains and are responsible for the hydrophobic properties of leaf waxes, acting as an external, environmental barrier (Jetter *et al*., 2006). This resistance to molecular alteration is provided by the lack of functional groups, as *n*-alkanes are straight-chain hydrocarbons, this allows *n*-alkanes to remain stable in sediments for tens of millions of years (Eglinton and Logan, 1991). The watershed plants, from which the organic material is derived, reflect the paleoenvironmental conditions of the sediments in which they were deposited through the geochemical signatures of these organics (Brincat, 2000). Thereby, *n*-alkanes extracted from soil samples act as proxies and can be used as indirect evidence to infer paleoclimate at the time of deposition.

This study represents environmental changes in lake sediments within the Great Basin of western North America. Along with molecular analyses, providing information of

terrestrial versus aquatic input, isotopic analysis was also conducted providing data for insight into paleoclimate. *N*-alkanes were isolated from four sediment samples to distinguish between both terrestrial vs. aquatic organic matter as well as the input of C_3 vs. C_4 plants. Terrestrial and aquatic matter was identified via various calculations based on GCMS analyses. C_3 and C_4 photosynthetic pathways were identified based on $\delta^{13}C$ values from GC-IRMS analyses.

Through carbon specific isotopic analyses, organic material of land plants with differing metabolic pathways can be identified (Meyers, 1994). Bulk carbon $\delta^{13}C$ values in C_3 and C_4 plants provide distinctly different signatures (Fig. 1). Preference for the lighter carbon isotope, Carbon-12, is stronger in C_3 plants than C_4 plants as a result of their photosynthetic processes, leading to differing isotope signatures. Specifically, $\delta^{13}C$ is depleted in C_3 plants, while the opposite is seen in C_4 plants (Smith and Epstein, 1971). The biological group, defined via these differing photosynthetic pathways, then allows for the paleoecology of the lake to be tied to environmental changes at the time of deposition. Shifts in biological groups of vegetation are a product of shifts in environment, which results in a C_3 vs. C_4 preference. The isotopic ratios that result from this preference of carbon isotopes depend on CO_2 content, which may vary due to atmospheric changes in CO_2 concentration or due to internal changes in CO_2 concentration in leaves caused by differences in leaf stromatal behavior. C_3 plants are most successful at high concentrations of CO_2 (*g*) and C_4 plants succeed with low concentrations of CO_2 (*g*) (Ehleringer *et al.,* 1997). C_4 plants tend to thrive in hot and arid conditions, while C_3 plants thrive in cooler, moister conditions. Most aquatic plants are C_3 plants (Farquhar *et al*., 1989).

C_3 plants also commonly represent trees and shrubs, typical of wooded areas. In wetter climates, these tend to dominate over C_4 plants, with some examples of C_3 plants including grasses and sedges (Eglington and Eglington, 2008). Although C_3 plants thrive in wetter areas they can also occur in arid conditions but this, too, can be distinguished. C_3 plants can be categorized into two types with respect to molecular chain length of their constituent leaf waxes, short and long. This allows the variations in chain lengths to be used to determine what biological group they originated from once their photosynthetic pathway has been determined via isotopic analysis. Long-chained *n*-alkanes result from C_3 plants growing in a savannah-like hot, arid environment and short-chained *n*-alkanes result from C_3 plants growing in a wetter rain-forest environment (Badewien *et al.*, 2015). Short-chained lipids are typical of algae, in this case to synthesize cell membranes. Long-chained lipids are typical of vascular plants to synthesize leaf waxes which are used for moisture regulation and increased rigidity.

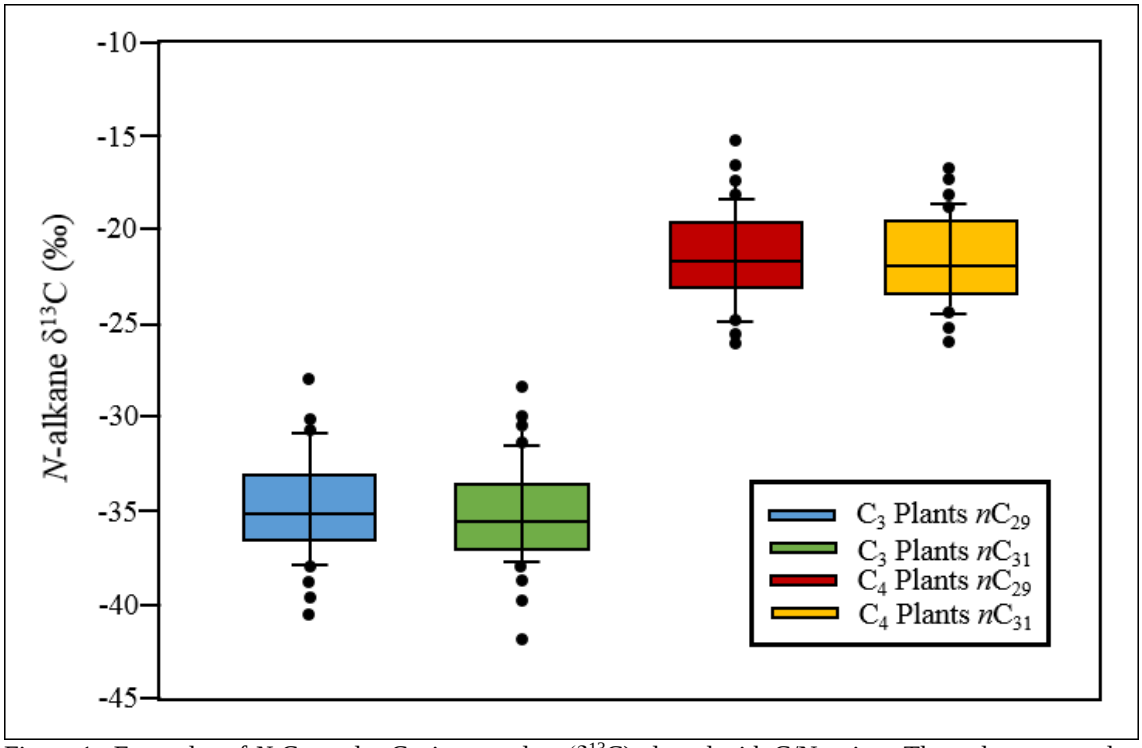

Figure 1. Examples of *N*-C_{29} and *n*-C_{31} isotope data ($\delta^{13}C$) plotted with C/N ratios. These data are used to distinguish between C_3 and C_4 plant types. This plot defines a carbon isotope value of approximately -27 to differentiate between C_3 and C_4 plant types (from Castañeda and Schouten, 2011).

2. Methods

2.1 Samples and Locations

The BB3-I sediment core was extracted from the western edge of Summer Lake, OR at 42.8057° N, 120.7831° W. Summer Lake is a remnant of the Pleistocene lake, Chewaucan (Fig. 2) (Licciardi, 2001). Modern Summer Lake is the largest of the four sub-basins associated with Lake Chewaucan and covers a 1243 km^2 (480 mi^2) area with an average depth of 0.30 meters (0.98 ft) and a maximum depth of 0.61 meters (2.0 ft) (Allison, 1982). Ancient Lake Chewaucan was a freshwater lake that spanned 461 mi^2 and reached depths up to 114 meters (374 ft) (Allison, 1982). Lake Chewaucan transformed from freshwater to saline water when the lake began to dry up at the end of the Pleistocene (Allison, 1982). Summer Lake is currently recharged by the spring-fed Ana River (Allison, 1982).

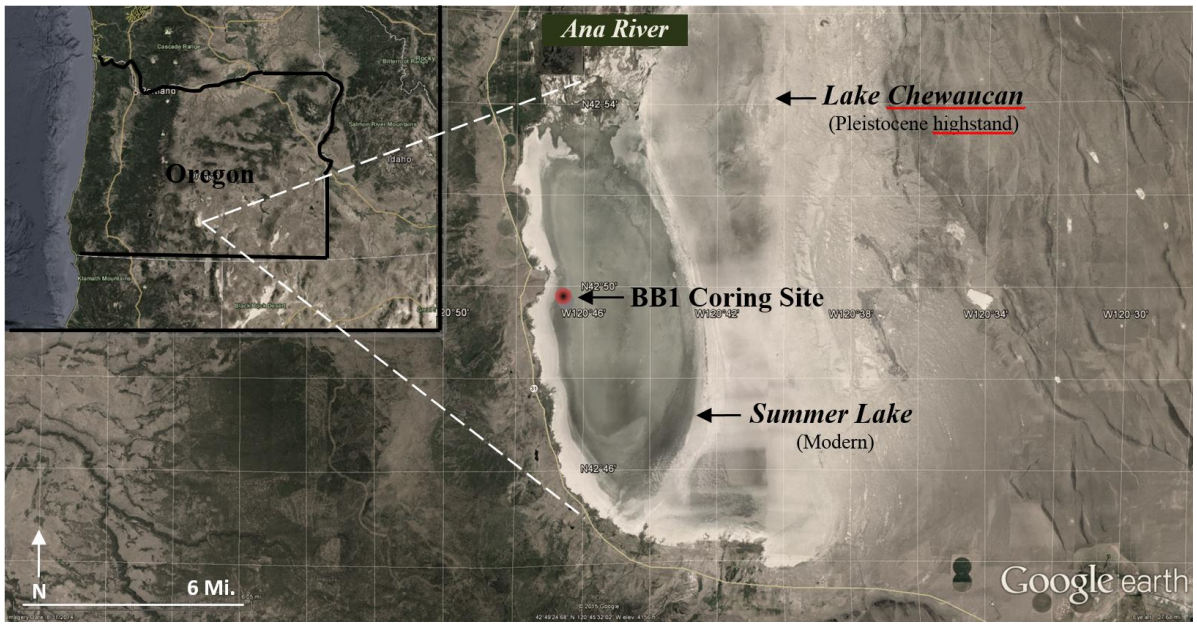

Figure 2. Base location map of Lake Chewaucan previous shoreline and its sub-basin, Summer Lake. Coring site of the Bed and Breakfast Core (BB3-I) is shown in red.

The coring site (Fig. 2) is located at the depocenter of the half-graben from which the basin formed and was obtained with a modified Livingston piston coring device in September 2010 (McCuan, 2011). The 11-cm diameter core was split in two parallel to the axis of the core, one to be archived and one for analysis. The segment of core analyzed in this study consists of a silty-clay and clay deposits. Due to previous analysis being done on this core, sediment for analysis was limited. Adding to this, the high silt content of the core resulted in a water to sediment weight ratio of approximately 1:1 and the organic content of the sediments was typically only 1%. Thus the samples, averaging 30g in size, were limited to one each from the two stadial and interstadial zones represented in Figure 3 (Thompson, 2014). These samples represent two meters of sediment, deposited over a four-thousand year interval and dating from approximately 38-35 ka. The ages of the sediments represented by the four samples were: 37.2 ka, 36.0 ka, 35.3 ka and 34.3 ka. Analyses on these samples consists of *n*-alkane molecular analysis and stable carbon isotope measurements.

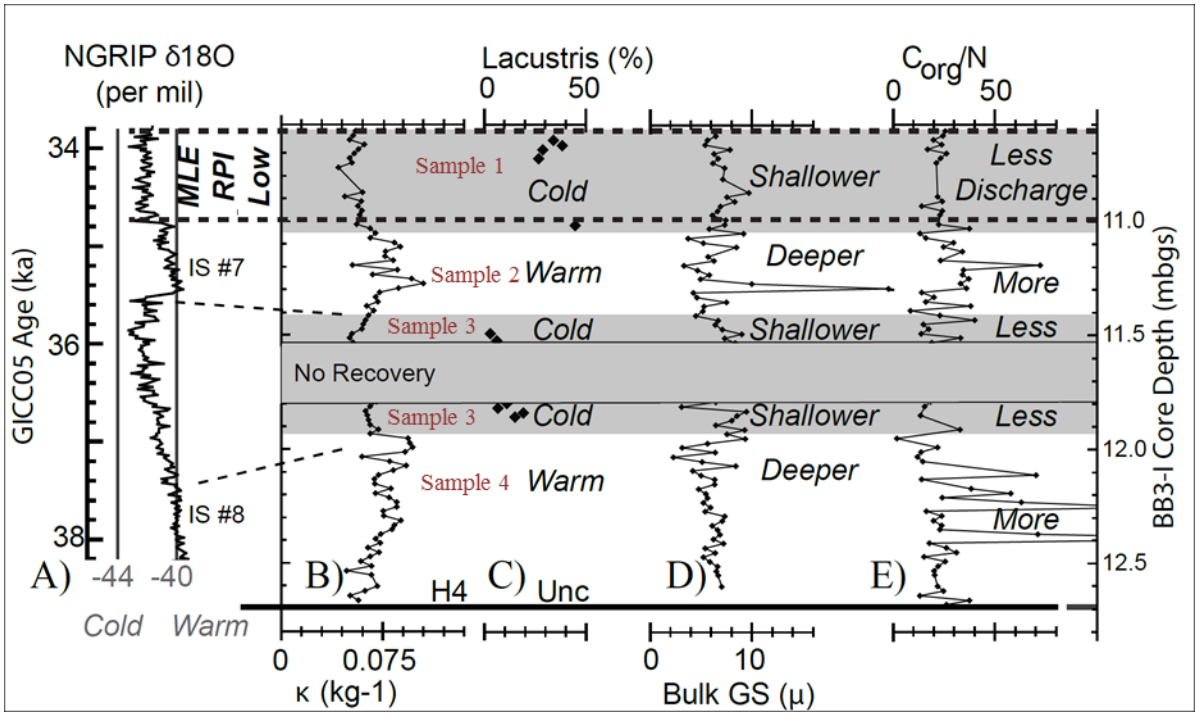

Figure 3. Sample locations, in red, taken from BB3-I Dansgaard-Oeschger interstadial (IS) and stadial events. Additional proxies, lacustris, bulk grain size, and C/N ratio are shown in correlation with NGRIP ice core $\delta^{18}O$. Grey backgrounds correspond with cold, shallow environments and white backgrounds correspond with warm, deep environments (modified from Zic *et al*., 2002; Thompson, 2014).

2.2 Lipid Extraction and Quantification

Sediment samples from the BB3-I core were sampled in approximately 11.0 g – 40.0 g amounts from the 10.5 mbgs – 12.5 mbgs core interval which ranged in age from 38-34 ka (Fig. 3). The samples were taken from the four intervals shown in Figure 3, at 10.7, 11.2, 11.5, and 12.3mbgs, respectively. These samples were then set in a desiccator to dry out in order to get a dry-sample weight (Table 1). Once dry, samples were weighed using an A&D GH Series Analytical Balance GH-252, crushed using a mortar and pestle and placed into 25 x 150 mm test tubes with Teflon-lined screw caps. Sample masses are listed in Table 1 of the appendix. Lipids were extracted from each sample with 50 ml of a 9:1 dichloromethane and methanol (DCM:MeOH, v:v) solvent at STP, and set on the lab quake to mix overnight.

Table 1. Original sample weight taken from BB3-I core and sample weight after placed in desiccator which resulted in an approximately 50% weight reduction.

Sample #	**Age *(Ka)***	**Depth *(mbgs)***	**Orig. Weight *(g)***	**Dry Weight *(g)***
1	34.4	10.7	82.04	32.048
2	35.3	11.2	27.67	11.20
3	36.0	11.5	75.60	39.49
4	37.2	12.3	53.74	31.12

Once extracted, the samples were rested for sedimentation. The supernatant was then removed and passed through a glass column. A 20 x 200 mm glass column was prepared with glass wool approximately ¼ full to filter out all sediment from flowing through.

The elution extract was concentrated to dryness with a rotovaporator (set at 50^{o}C). The extract was then transferred from the round bottom flask into a smaller 13 x 100 mm test tube. A centrifuge, set at 2800 rpm for ten minutes, was used to separate any remaining sediment that may have gone through the glass wool filter. With the sediment settled at the bottom of the test tube, top portion of the sample is transferred into a new test tube. This test tube is then placed into the centrivap to further concentrate down to dryness at 50^{o}C.

Column chromatography was set up using a glass pipette to separate the non-polar, saturated *n*-alkanes, from polar lipids. Glass wool was compacted into the base of a Pasteur pipette to plug the tip and act as a sediment filter. A thin layer of wash sand was placed on top of the glass wool and the column was filled the rest of the way with silver nitrate-impregnated silica eluted with hexane (9:1, silica gel: silver-nitrate powder). The column was then equilibrated with hexanes and the saturated lipids in the extract were eluted with 2 mL of hexane. The test tube used to collect the sample was then placed into the centrivap to

concentrate down to dryness. From the centrivap, samples were transferred into 2 mL HPLC vials and filled up with 1 ML of solvent.

These samples were then run on the GC-2010 Plus, a multi-dimensional GCMS system that performs separations using two columns of different chromatographic selectivity. The samples were analyzed with a Restek Rxi-5Sil MS (30 m long, 0.25mm internal diameter) with a 0.25 μm bonded phase column. The GC method used in this *n*-alkane analysis contained a ramp rate of 6.0 ^{o}C/min, starting at 60^{o}C, ending at 300^{o}C, a holding time of 10 min, 290^{o}C inlet temperature, a splitless constant flow rate set at 1.2 mL/min and an injection volume of 1.5 μL. An *n*-alkane standard calibration curve was created for quantification. The standards were prepared with the target compounds, C_{21}-C_{36} *n*-alkanes. Solutions of 0.001 mg/mL, 0.01 mg/mL and 0.1 mg/mL concentrations were mixed and each run on the GCMS at the respective ramp up rate and temperature to construct a calibration curve prior to running the samples. Creating a standard calibration curve allowed for the relationship between peak areas and analyte concentration to be determined. Each sample was run in triplicate and measurements containing a margin of error greater than 40% were deemed as outliers and not used in calculations.

2.3 Sediment Carbon Content and Isotope Analysis

Following the molecular analysis carried out at CSU Bakersfield, these samples were sent to Southeast Environmental Research Center Stable Isotope Laboratory at Florida International University for stable organic carbon isotope ratio analysis. The machine used for this analysis was a Finnigan *Delta* Plus GC-IRMS.

3. Results and Discussion

3.1 N-Alkane Concentrations

The *n*-alkane area data are presented in Table 2 and the corresponding concentration data are presented in Table 3 (Reagan, 2015). The concentration is listed as µg of lipid *n*-alkane extract per gram of dry weight sediment. These conversion equations are listed in Table 4, where Y is the area input and X is the concentration output. These intercept values were provided by each respective *n*-alkane standard. This data allowed for a comparison between concentration and depth. The concentration of lipid extract is highest towards the bottom of the core reaching 291.5 µg/g.

Table 2. Sample specific *N*-alkane area values from GC-MS analysis.

Sample #	**C_{22} Area**	**C_{23} Area**	**C_{24} Area**	**C_{25} Area**	**C_{26} Area**	**C_{27} Area**	**C_{28} Area**
1	371,038	914,367	804,279	961,407	419,712	634,138	139,185
2	128,695	128,695	216,772	578,420	229,284	1,189,043	314,466
3	9,703	23,604	15,173	37,379	25,694	693,729	26,118
4	-	-	-	-	-	1,623,076	-

Sample #	**C_{29} Area**	**C_{30} Area**	**C_{31} Area**	**C_{32} Area**	**C_{33} Area**	**C_{34} Area**	**C_{35} Area**	**C_{36} Area**
1	416,348	51,619	113,792	729	23,173	631	3,786	-
2	2,111,399	245,001	1,506,603	133,427	307,434	87,220	65,527	2,421
3	1,013,268	15,775	690,119	13,181	197,316	7,059	57,240	-
4	1,776,647	-	1,008,694	-	150,913	-	-	-

Table 3. *N*-alkane concentration values calculated from area.

Sample #	Depth *(mbgs)*	Age *(ka)*	C_{22} *µg/g*	C_{23} *µg/g*	C_{24} *µg/g*	C_{25} *µg/g*	C_{26} *µg/g*	C_{27} *µg/g*	C_{28} *µg/g*
1	10.7	34.3	66.59	116.3	106.20	120.6	71.04	90.67	47.90
2	11.3	35.3	11.72	17.85	14.54	26.10	14.94	45.63	19.30
3	11.5	36.0	10.56	10.56	10.56	10.56	10.56	154.8	10.77
4	12.3	37.2	-	-	-	-	-	145.2	-

Sample #	Depth *(mbgs)*	Age *(ka)*	C_{29} *µg/g*	C_{30} *µg/g*	C_{31} *µg/g*	C_{32} *µg/g*	C_{33} *µg/g*	C_{34} *µg/g*	C_{35} *µg/g*	C_{36} *µg/g*
1	10.7	34.3	89.08	54.92	85.32	51.27	75.04	67.74	71.55	69.27
2	11.3	35.3	103.2	24.05	114.1	21.18	55.94	29.85	29.93	16.65
3	11.5	36.0	233.3	15.22	205.3	16.55	76.70	21.83	22.42	22.42
4	12.3	37.2	233.5	-	291.5	-	227.8	-	184.7	-

Table 4. *N*-alkane calibration equations taken from GC-MS machine following analysis of standards.

Calibration Alkane Equations					
C_{27}	Y=	3.601e+008x - 118839.5	C_{28}	Y=	3.049e+008x - 105494.1
C_{29}	Y=	2.493e+008x - 92148.8	C_{30}	Y=	2.096e+008x - 102539.3
C_{31}	Y=	1.700e+008x - 112929.8	C_{32}	Y=	5.101e+0075x - 85785.1
C_{33}	Y=	8.502e+007x - 58640.4	C_{34}	Y=	6.912e+007x - 48493.2
C_{35}	Y=	5.322e+007x - 38346.0	C_{36}	Y=	5.322e+007x - 38346.0

3.2 Possible Climate Impacts on Molecular Chain Length Distribution.

The concentrations of odd vs. even and long v. short *n*-alkanes are plotted in Figures 4-7. Odd-chain *n*-alkane concentrations generally increase in concentration with age (Fig. 4). As expected, the even-chained *n*-alkanes, $nC_{22\text{-}36,}$ correspondingly decrease with age (Fig. 5). This relationship may be indicative of an increase in terrestrial plant input into the lake with age (Bush and McInery, 2013). The major *n*-alkanes in sediment samples 4-2 are C_{31} and C_{29}, both being long, odd *n*-alkanes, and are indicative of a terrestrial environment. In interstadial samples 4 and 2, C_{31} is more prominent than C_{29} and the opposite is seen in stadial samples 3 and 1. In stadial sample 1, the concentration of *n*-alkanes, as a whole,

decreases with the shorter *n*-alkanes, with C_{23} and C_{25} being the highest. The molecular distribution of *n*-alkanes shows a significant odd-to-even carbon preference in samples 4-2, which is typical in plants (Street, 2013). This is consistent with a study done by Rao *et al.* (2009), which concluded this finding to be a result of paleovegetational evolution. According to Rao *et al*. (2009) plants with a high *n*-$C_{27,29}$ content are indicative of a woody, forest environment and plants with a high *n*-C_{31} content are indicative of herbaceous, grassland environments.

The concentrations of long vs. short *n*-alkanes are plotted in Figures 6 and 7. Long chained *n*-alkanes increased in concentration with age while short chained *n*-alkanes decreased in concentration with age, indicating an inverse relationship. These data act in conjunction with the odd vs. even comparison to support a terrestrial environment in older sediment samples. Chain length is driven primarily by differences in vegetation types in terrigenous leaf lipids; forest leaf lipids contain smaller chain lengths than grass leaf lipids (Jeng, 2006). Samples 4, 3 and 2 all contain high concentrations of long chain *n*-alkanes $C_{27,29\ \&31.}$ A study carried out by Poynter *et al*. (1989) suggests that warmer climates contain plants that produce longer-chained *n*-alkanes. Samples 4 and 2 both contain higher concentrations of C_{31} than any other *n*-alkane. Another study, by Simoneit *et al*. (1991), supports these findings, with the C_{31} *n*-alkane found to be dominant in warm-climate areas. Carbon nitrogen data from samples 4-1 support this finding. C_{org}/N ratios contain a threshold of approximately 25, indicating a strong terrestrial input in samples greater than 25. As shown in Figure 8, samples 4 and 2 contain C_{org}/N data representative of a warmer climate while the opposite is seen in samples 3 and 1.

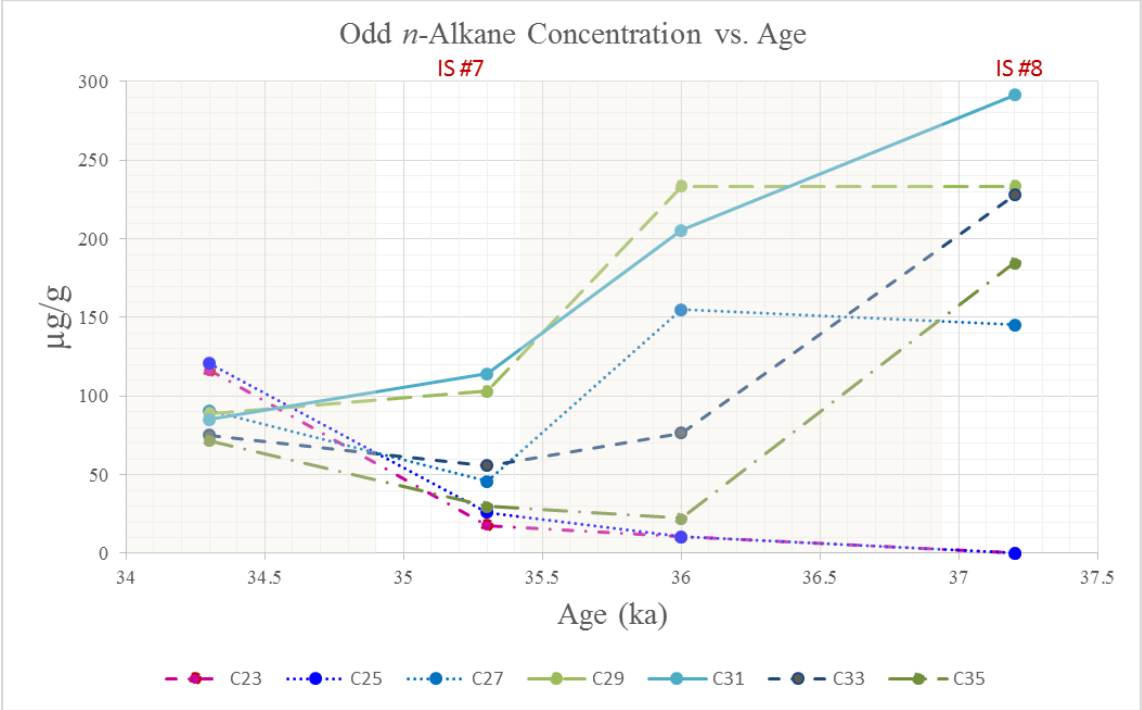

Figure 4. Odd chain *n*-alkane concentration (µg/g) vs. age (ka). In the oldest three sediment samples, *n*-$C_{29\&31}$ are the dominant *n*-alkanes and in the youngest sample *n*-$C_{23\&25}$ are the dominant *n*-alkanes. An increase in odd-chain *n*-alkanes is representative of terrestrial organisms.

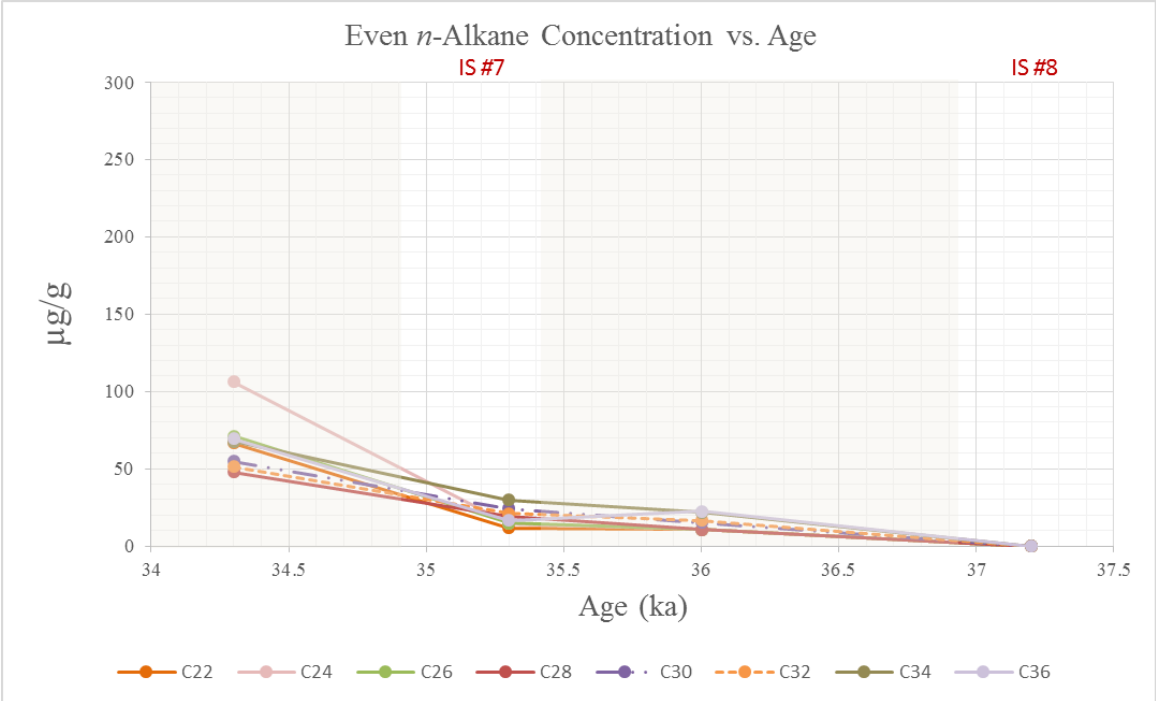

Figure 5. Even chain *n*-alkane concentration (µg/g) vs. age (ka). Very low concentrations of even *n*-alkanes are present in the oldest three samples while they have been determined to be approximately equal to odd *n*-alkanes in the youngest sample. An increase in even-chain *n*-alkanes is representative of aquatic organisms.

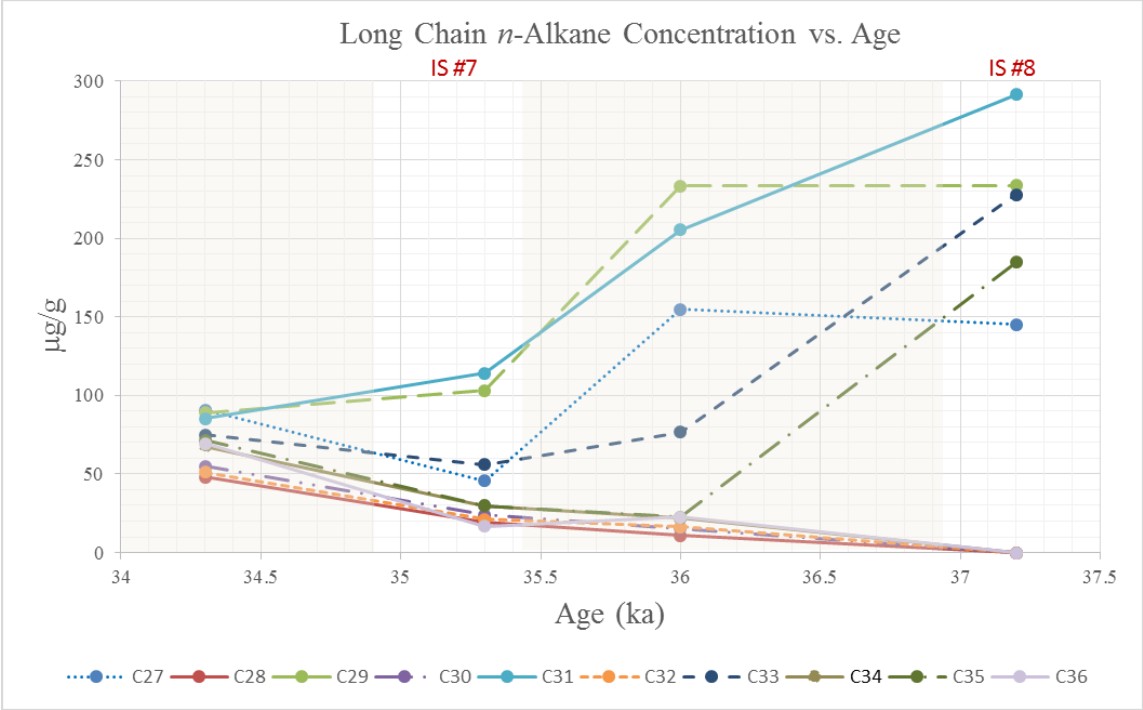

Figure 6. Long-chain *n*-alkane concentration (µg/g) vs. age (ka). Long-chain *n*-alkanes increase with increase in age showing a positive relationship. An increase in long-chain *n*-alkanes is representative of terrestrial organisms.

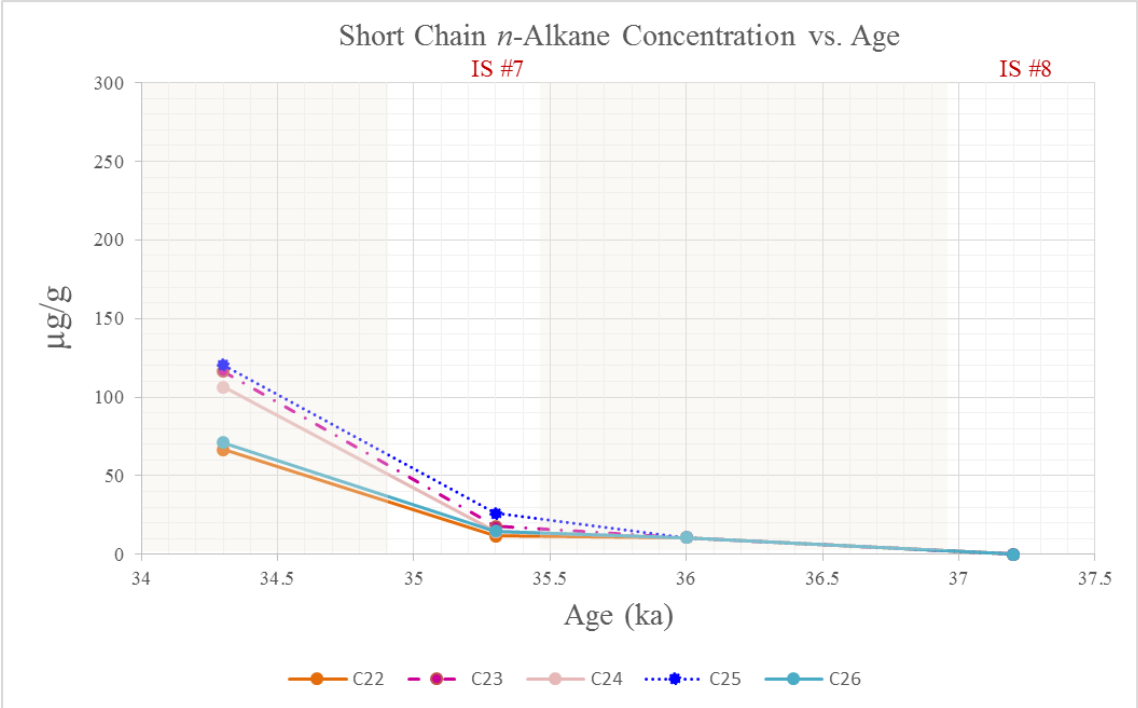

Figure 7. Short-chain *n*-alkane concentration (µg/g) vs. age (ka). Short-chain *n*-alkanes decrease with increase in age. An increase in short-chain *n*-alkanes is representative of aquatic organisms.

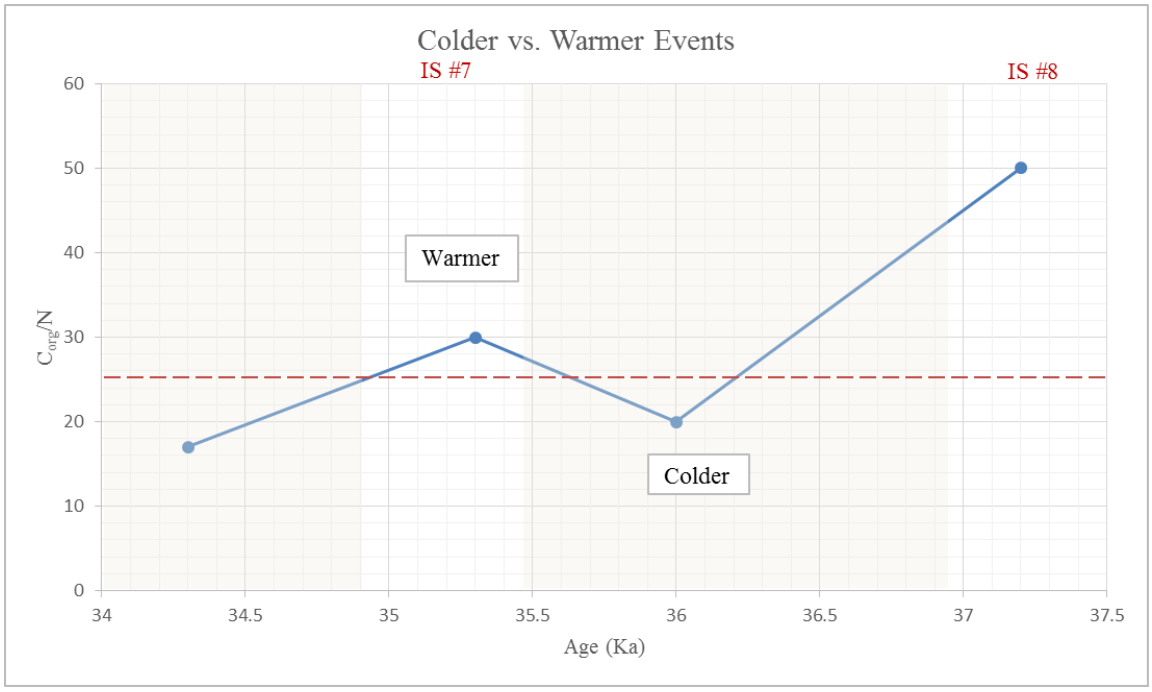

Figure 8. According to Lamb *et al.* (2006) C_{org}/N ratios can also indicate freshwater vs. terrestrial plants as freshwater plants contain a smaller ratio, between 4-10 and terrestrial plants contain a higher ratio, typically 15 and above (Meyers and Teranes, 2001). C_{org}/N data is plotted with age (ka) showing a threshold ratio of 25, indicated by the dotted line in red. This threshold is used to define lower vegetation input during colder, stadial events and higher vegetation input during warmer, interstadial events (modified from Thompson, 2014).

3.3 ACL, CPI and P_{aq} Values

Three calculated indices were used to infer paleoecology with the *n*-alkane data from GCMS analysis. This includes: Average Chain Length (ACL), Carbon Preference Index (CPI), and the contribution of aquatic plants (P_{aq}).

Average chain length, Equation 1, was used to calculate the weight-averaged number of carbon atoms per molecule in higher plants, which range from C_{25} to C_{33} in *n*-alkanes. *N*-Alkane chain lengths in samples 4-1 ranged from C_{21} to C_{36}, although they are not all used to calculate ACL. The shorter-chain *n*-alkanes are excluded in Equation 1 because they are not representative of terrestrial environments. The largest ACL values are seen in samples 2-4, 29.83, 29.61 and 30.31, respectively (Fig. 9). Notably, the two highest values are from the interstadial samples. Due to terrestrial organisms containing a larger ACL than those of

aquatic organisms, this finding remains consistent with the finding based on concentration data. Although the data presented in Figure 9 represents aquatic vs. terrestrial organisms, the difference is minor with this calculation and is better represented in Figures 6 and 7.

$$ACL_{25\text{-}33} = \frac{25C_{25}+27C_{27}+29C_{29}+31C_{31}+33C_{33}}{C_{25}+C_{27}+C_{29}+C_{31}+C_{33}} \qquad ACL = \frac{\sum(iX_i)}{\sum X_i} \qquad (1)$$

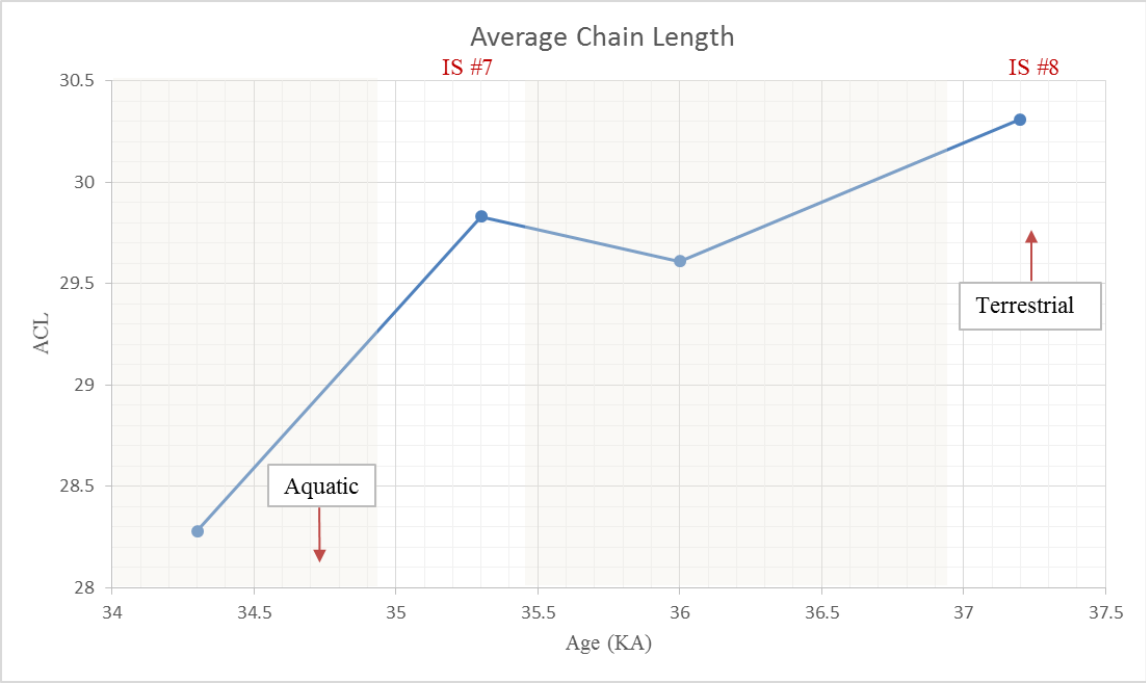

Figure 9. Average chain length of samples showing that the three oldest samples contain implications of terrestrial plant types while the youngest sample is trending toward aquatic plant types.

Both odd and even N-alkanes were used to determine the Carbon Preference Index (CPI), calculated as shown in Equation 2. *N*-alkane concentration extracted from soil samples ranged from 10.56 to 1294 µg/g with an average of 183.2 µg/g (Fig. 10). The CPI is used to determine terrestrial input history; CPI values greater than 1 are indicative of terrestrial plants, which average approximately 10.5 when directly sampled (Bush and McInerney, 2015). Again, the two highest values are from the interstadial sediment samples.

$$\text{CPI} = \frac{\sum(\Sigma_i + X_{i+1} + \ldots X_n) + \sum(X_{i+2} + \ldots + X_{n+2})}{2\ X\ \sum(x_{i+1} + \ldots + X_{n+1})} \quad \text{or} \quad \frac{\Sigma_{ODD}\,(C_{21-35}) + \Sigma_{ODD}\,(C_{23-35})}{2 \times \Sigma_{EVEN}\,(C_{22-36})} \qquad (2)$$

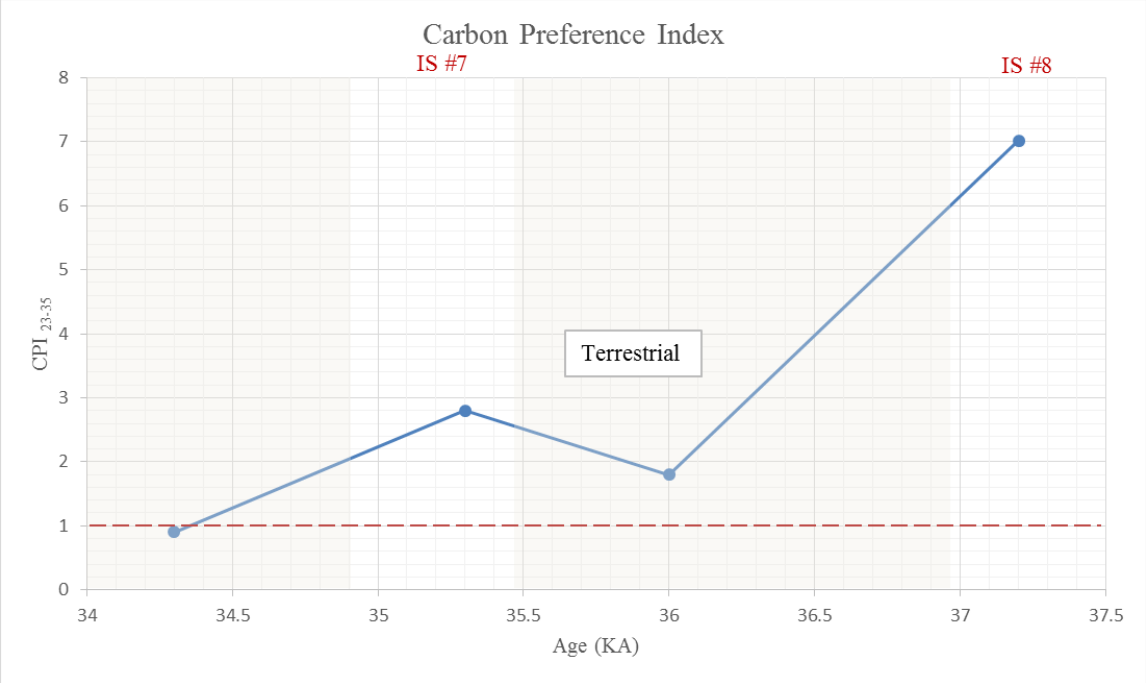

Figure 10. The relative contribution of aquatic plants versus terrestrial plants (P_{aq}). Interstadial samples 4 and 2 and stadial sample 3 are in the terrestrial range. As with the ACL index (Figure 9), the interstadial samples have the highest tendency towards terrestrial vegetation. Stadial sample 1 falls in the non-terrestrial range.

The relative contribution of aquatic plants was determined using Equation 3 and the results are shown in Fig. 11. This calculation shows a contrast between aquatic and terrestrial plants due to aquatic plants containing a shorter-chain *n*-alkane dominance than terrestrial plants, which are dominated by mid to longer chain *n*-alkanes. Samples 4-2 reflect values that indicate a terrestrial origin. In contrast, sample 1 reflects a more aquatic organism. Again, the two interstadial samples reflect the most contributions from terrestrial vegetation.

P_{aq} and CPI values display an inverse relationship, as expected. CPI values for samples 2-4 are 2.80,1.80, and 7.02, respectively and remain above the threshold for aquatic plants. Stadial sample 1, from 34.3 Ka contains a CPI of 0.900, being slightly below the

terrestrial-aquatic barrier this sample represents an aquatic environment. This is supported by inverse P_{aq} values (Fig. 11). Sample 4 from 37.2 Ka is in the terrestrial range below 0.090 at 0.046. Stadial sample 3 and interstadial sample 2 taken from mid-core, 36.0 and 35.5 are 0.21 and 0.17, respectively. These mid-core samples are both in the emergent range. This observation is suggestive of a slight increase of aquatic input into a terrestrial dominated environment.

$$P_{aq} = \frac{C_{23}+C_{25}}{C_{23}+C_{25}+C_{29}+C_{31}} \quad (3)$$

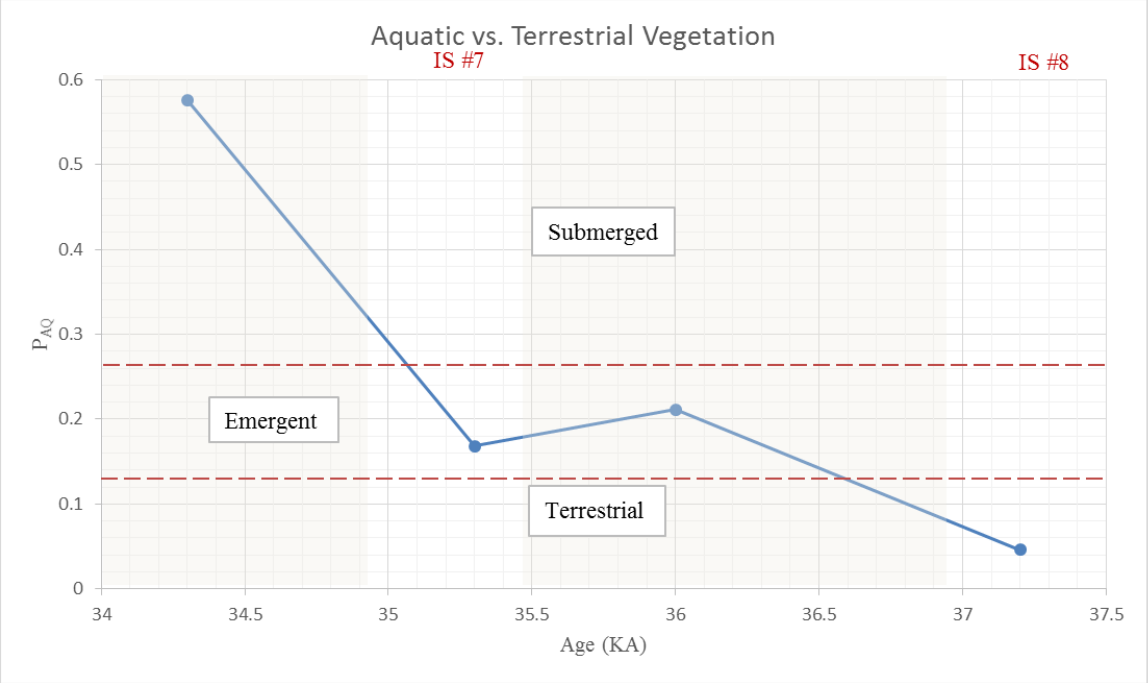

Figure 11. P_{aq} values compare aquatic vegetation to terrestrial vegetation. Interstadial sample 4 is in the terrestrial range. Both stadial sample 3 and interstadial sample 2 are in the emergent range. Stadial sample 1 is well within the submerged range.

3.4 Carbon Fixation Pathways Provided by Carbon Isotope Ratios

C_3 and C_4 photosynthetic pathways are both useful in relation to global changes due to their different responses to temperature and carbon dioxide (CO_2) concentrations. In high CO_2 concentrations, or when conditions are moist or cool, plants open their stromatal to maintain higher internal leaf CO_2 concentrations, allowing C_3 plants to thrive. In contrast, C_4 plants thrive when CO_2 values are low, either due to low atmostpheric CO_2 or due to conditions, such as being hot and dry, encouraging stromatal closure and low internal leaf CO_2 concentrations (Ehleringer and Cerling, 2002).

C_3 and C_4 plant types can be distinguished through their carbon isotope ratios, $^{13}C/^{12}C$. Carbon isotopes, $\delta^{13}C$, are presented in permille (‰) and are relative to the Pedee Belemnite international standard (VPDB) (Equation 4). GCMS results, shown in Figure 12A, were used to calibrate Isotope results, shown in Figure 12B. Carbon fixation processes, especially the enzymes associated with the fixation of atmospheric carbon, dictate this characterization, which is approximately -27 ± 2.0 ‰ for C_3 plants and approximately -13 ± 1.2 ‰ for C_4 plants (Tieszen, 1991). A more specific analysis of carbon isotope ratios by Kohn, 2010 resulted in isotope compositions ranging from -32.6 to -19.2‰ and averaged -29.6 ± 1.9‰ for C_3 plants and -16.6 to -10.4‰ with an average of -12.7 ± 1.4‰ in C_4 plants.

$$\delta = \left[\frac{\left[\frac{^{13}C}{^{12}C}\right]_{sample}}{\left[\frac{^{13}C}{^{12}C}\right]_{standard}} - 1 \right] \times 1000 \qquad (4)$$

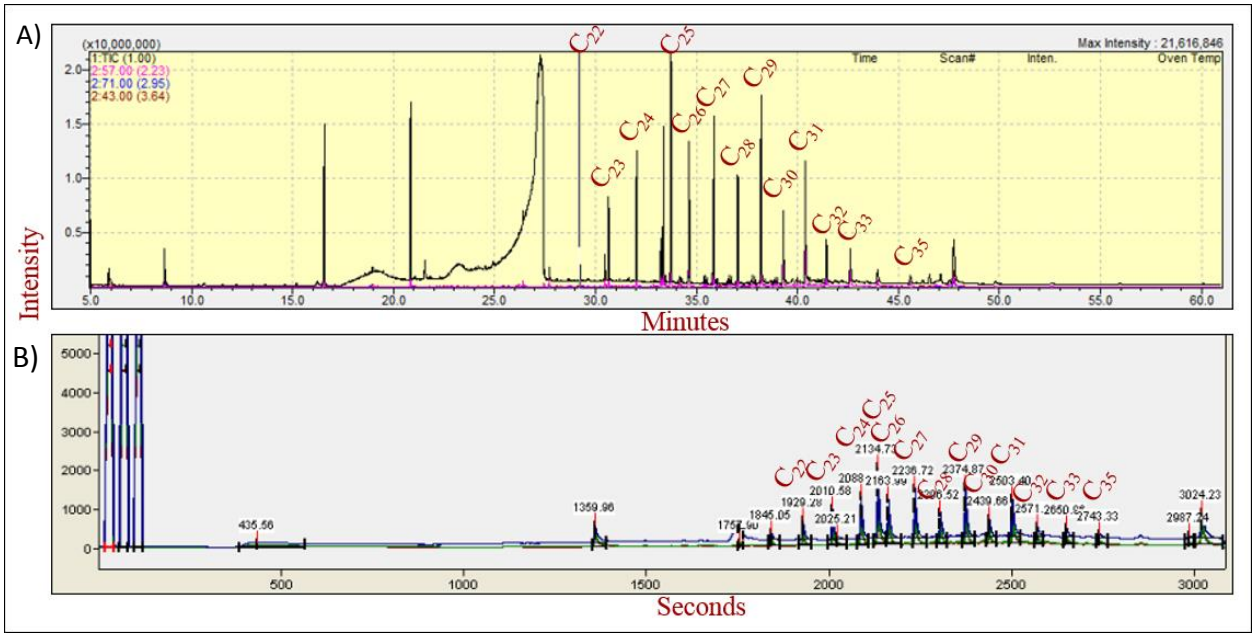

Figure 12. A) GCMS results used to determine *n*-alkanes in B) IRMS analysis. Peaks correlated with specific *n*-alkanes from GCMS analyses were used to determine *n*-alkanes from IRMS analyses.

Isotopic analysis of the BB3-I core provided evidence of abundant C_3 plants (Ehleringer and Cerling, 2002). Isotope ratios ranged from -24.50 ‰ to -42.45 ‰ indicating that all plants followed the C_3 photosynthetic pathway (Fig. 13). High $\delta^{13}C$ signatures are also a typical physiological response to arid environmental conditions (Kohn, 2010). Values that could not be correlated with specific *n*-alkanes from previous GC-MS analysis were excluded from this graph. The values used are listed in Table 5.

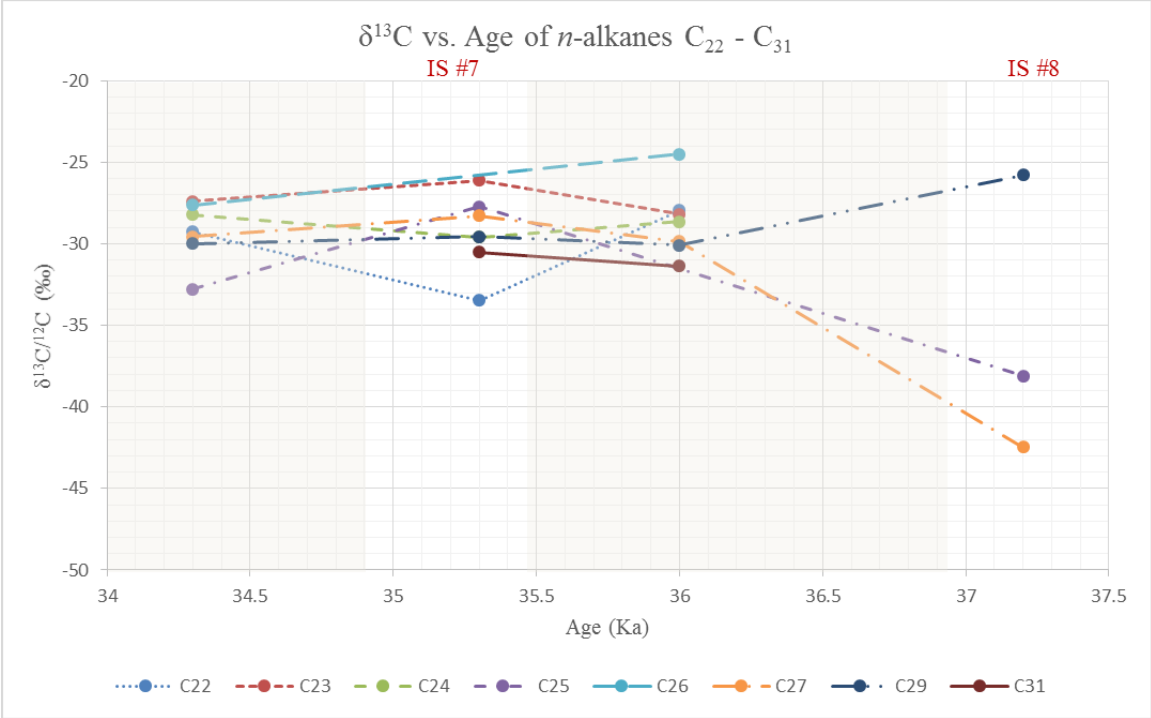

Figure 13. Carbon specific isotope ratios for each sample. Due to the low isotopic ratio, all four samples fall in the C_3 vegetation range.

Table 5. Photosynthetic pathways based on carbon specific isotope ratios. The low isotopic signatures correspond with C_3 vegetation. The very low isotopic signatures correspond with a possible canopy effect.

***N*-alkane Specific Carbon Isotope Data**

***N*-alkane**	**Depth** (mbgs)	**Age** (ka)	**RT** (s)	**$\delta^{13}C$ / ^{12}C** (‰, VPDB)	Photosynthetic Pathway
C_{22}	10.7	34.3	1928.7	-29.276	C_3
	11.2	35.3	1928.7	-33.471	C_3
	11.5	36.0	1928.7	-27.939	C_3
C_{23}	10.7	34.3	2009.7	-27.406	C_3
	11.2	35.3	2013.9	-26.129	C_3
	11.5	36.0	2010.0	-28.175	C_3
C_{24}	10.7	34.3	2087.9	-28.229	C_3
	11.2	35.3	2087.9	-29.594	C_3
	11.5	36.0	2088.1	-28.644	C_3
C_{25}	10.7	34.3	2133.5	-32.773	C_3
	11.2	35.3	2134.9	-27.716	C_3
	12.3	37.2	2133.7	-38.109	C_3
C_{26}	10.7	34.3	2163.1	-27.616	C_3
	11.5	36.0	2163.1	-24.503	C_3
C_{27}	10.7	34.3	2235.9	-29.553	C_3
	11.2	35.3	2235.9	-28.269	C_3
	11.5	36.0	2236.1	-29.872	C_3
	12.3	37.2	2235.9	-42.454	C_3 - Canopy Effect
C_{29}	10.7	34.3	2373.6	-29.999	C_3
	11.2	35.3	2373.6	-29.552	C_3
	11.5	36.0	2373.8	-30.083	C_3
	12.3	37.2	2369.4	-28.796	C_3
C_{31}	11.2	35.3	2502.8	-30.503	C_3
	11.5	36.0	2502.8	-31.358	C_3

3.5 Isotope Data and C_{org}/N Ratio of Organic Matter from Sediment

Fluctuations in C_{org}/N ratios act as indicators of algal versus land-based time periods. An understanding of this ratio leads to information regarding lake high-stand versus low-stand periods. According to Lamb *et al*. (2006) C_{org}/N ratios indicate freshwater vs.

terrestrial plants. Freshwater plants contain a smaller ratio, between 4 and 10, and terrestrial plants contain a higher ratio, typically 15 and above (Meyers and Teranes, 2001). Kirby (2012) and Thompson (2014) used this ratio in conjunction with higher grain-size in the coarse grain fraction to suggest that higher terrestrial-based content occurs with greater stream discharge due to greater transport of terrestrial plant matter into the lake.

C_{org}/N ratios determined by Thompson (2014) were used as reference for comparison with isotope data. The C_{org}/N ratios for samples 1-4 are 17, 30, 20, and 50, respectively. These results indicate that this core interval contains predominately terrestrial plants due to the high C_{org}/N ratio remaining above 20 in samples 2-4 (Fig. 8) (Meyers and Lallier-Verges, 1999). The low nitrogen content is due to the presence of lignin and cellulose (Lamb *et al*., 2006). Due to the shallowest sample containing a C_{org}/N ratio of 17, which is below the barrier of 20 that is representative of terrestrial vegetation, it was considered to be of non-terrestrial origin.

Carbon specific isotope data and C_{org}/N (see Figure 8) are plotted in Figure 14; this comparison provides a direct indication that none of the four samples fall within the C_4 photosynthetic pathway. Due to the lowered C_{org}/N ratio, samples one and three (from the stadial zones) fell within or very close to the lacustrine algae range as expected. Samples that have very negative values, i.e. with $\delta^{13}C$ values below -32, are likely the results of canopy effects (Kohn, 2010) (Fig. 14). Values are very negative for C_3 plants growing in the shaded understory of forests due to photosynthesis occurring in low light and the "recycling" of CO_2 that is released by plants near ground level during plant respiration.

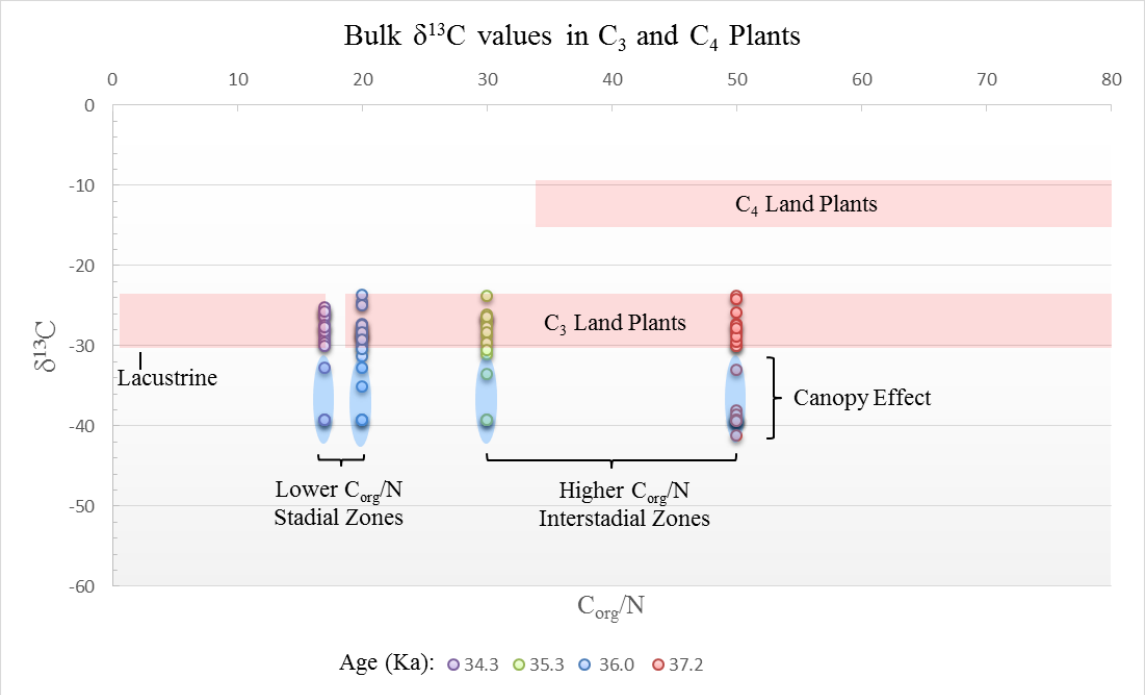

Figure 14. Higher isotope ratios are indicative of C_4 vegetation while lower isotope ratios are indicative of C_3 vegetation (Meyer and Lallier-Verges, 1999). Samples 1-4 were all in the C_3 range hence, no C_4 vegetation was present. Sample 1, shown in purple, has a low C/N and isotope ratio. The low C/N ratio indicates an algal origin. Samples circles in blue contain a very negative isotope ratio, representative of a canopy effect (i.e. understory plants growing in the shade of other plants).

4. Conclusions

For the interval of the BB3-I core analyzed in this study all three *n*-alkane indices (ACL, CPI, and P_{aq}) suggest a higher terrestrial vegetation input into the lake during warm interstadials (Figure 8) from Thompson (2014). It was also noted that interstadial samples 4 and 2 both contain higher concentrations of *n*-C_{31}, which is preferentially seen in graminoids (grasses) while stadial sample 3 contains *n*-C_{29} in higher concentrations, which is indicative of woody plants. Collectively, the above set of observations supports the teleconnection hypothesis of Benson *et al.* (1997) and several others summarized above wherein interstadial periods on millennial time scales during the Wisconsin glaciation are associated with wetter

climates in the Great Basin. High isotopic ratios ranging from -20.65 to -55.27, suggest that all organic matter is associated with C_3 plants (Ehleringer and Cerling, 2002)(Fig. 13).

References

Allison, I.S., 1982. Geology of Pluvial Lake Chewaucan, Lake Country, Oregon: Corvallis, OR, Oregon State University Press, vol. 11, pp. 1-5.

Badewien, T., Vogts, A., and Rullkotter, J., 2015. *N*-Alkane Distribution and Carbon Stable Isotope Composition in Leaf Waxes of C_3 and C_4 Plants from Angola: Organic Geochemistry, vol. 90, pp. 71-79.

Brincat, D., Yamada, K., Ishiwatari, R., Uemura, H., Naraoka, H., 2000. Molecular-Isotopic Stratigraphy of Long-Chain *n*-alkanes in Lake Baikal Holocene and Glacial age Sediments: Organic Geochmistry, vol. 31, pp. 287-294.

Bush, R.T., McInerney, F.A., 2013. Leaf wax *n*-alkane Distributions in and Across Modern Plants: Implications for Paleoecology and Chemotaxonomy: Geochimica et Cosmochimica Acta, vol. 117, pp. 161-179.

Bush, R.T., McInerney, F.A., 2015. Influence of Temperature and C_4 Abundance on *n*-alkane chain length distributions across the central USA: Organic Geochemistry, vol. 79, pp. 65-73.

Castañeda, I.S., and Schouten, S., 2011. A review of molecular organic proxies for examining modern and ancient lacustrine environments: Quaternary Science Reviews, vol. 30, pp. 2851-2891.

Eglinton G. and Logan G. A., 1991. Molecular preservation: Phil. Trans. Roy. Soc. London B: Biological Sciences, vol. 333(1268), pp. 315–328.

Ehleringer, J.R., and Cerling, T.E., 2002. C_3 and C_4 Photosynthesis: Encyclopedia of Global and Environmental Change, vol. 2, pp. 186-190.

Farquhar, G.D., Ehleringer, J.R., and Hubick, K.T., 1989. Carbon isotope discrimination and photosynthesis. Annual Review of Plant Biology, vol. 40(1), pp. 503-537.

Jeng, W.L., 2006. Higher plant *n*-alkane average chain length as an indicator of petrogenic hydrocarbon contamination in marine sediments. Marine Chemistry, vol. 102, pp. 242-251.

Jetter R., Kunst L. and Samuels A. L., 2006. Composition of plant cuticular waxes. In Biology of the Plant Cuticle (eds. M. Riederer and C. Muller). Blackwell Publishing, Oxford.

Kohn, M. J., 2010. Carbon isotope compositions of terrestrial C_3 plants as indicators of (paleo)ecology and (paleo)climate. Proceedings of the National Academy of Sciences of the United States of America, vol. 107(46), pp. 19691–19695.

Lamb, A.L., Wilson G.P., and Leng, M.J., 2006. A review of costal paleoclimate and relative sea-level reconstructions using $\delta^{13}C$ and C/N ratios in organic material. Earth-Science Reviews vol. 75, pp. 29-57.

Licciardi, J. M. 2001. Chronology of latest Pleistocene lake-level fluctuations in the pluvial Lake Chewaucan basin, Oregon, USA. J. Quaternary Sci., vol. 16, pp. 545–553.

McCuan, D.T., 2011. Late Pleistocene Geomagnetic Field Recorded in Sediments from the Depocenter of Pluvial Lake Chewaucan, Lake County, OR: A thesis submitted to the Department of Geological Sciences, California State University, Bakersfield.

Meyers, P.A., 1994 Preservation of elemental and isotopic source identification of sedimentary organic matter. Chemical Geology, vol. 144, pp. 289-302.

Meyers, P.A., and Lallier-Verges, E., 1999. Lacustrine Sedimentary Organic Matter Records of Late Quaternary Paleoclimates, Journal of Paleolimnology 21, pp. 345-372.

Negrini, R.M., Erbes, D., Faber, K., Herrera, A., Roberts, A., Cohen, A. and Foit, F., 2000. A paleoclimate record for the past 250,000 years from Summer Lake, Oregon, USA. 1. Chronology and magnetic proxies for lake level: Journal Paleolimnology, vol. 24, pp. 125-149.

Poynter, J.G., Farrimond, P., Robinson, N., Eglinton, G., 1989. Aeolian-derived higher plant lipids in the marine sedimentary record: links with paleoclimate. In: Leinen, M., Sarnthein, M. (Eds.), Paleoclimatology and Paleometeorology: Modern and Past Patterns of Global Atmospheric Transport: Dordrecht (Kluwer Academic Press), Hingham, Mass, pp. 435–462.

Rao, Z., Zhu, Z., Wang, S., Jia, G., Qiang, M., and Wu, Y. 2009. CPI values of terrestrial higher plant-derived long-chain n-alkanes: a potential paleoclimatic proxy: Frontiers of Earth Science in China, vol. 3(3), pp. 266-272.

Reagan, J., 2015. N-alkanes as Biomarkers for Latest Pleistocene and Holocene Precipitation in Cores from Tulare Lake, CA, U.S.A. A thesis submitted to the Department of Geological Sciences, California State University, Bakersfield.

Simoneit, B.R.T., Sheng, G., Chen, X., Fu, J., Zhang, J., Xu, Y., 1991. Molecular marker study of extractable organic matter in aerosols from urban areas of China: Atmospheric Environment, vol. 25A, pp. 2111–2129.

Smith, B.N., and Epstein, S., 1971. Two Categories of $^{13}C/^{12}C$ Ratios for Higher Plants: Plant Physiol. vol. 47, pp. 380-384.

Street, J.H., Anderson, R.S., Rosenbauer, R.J., Paytan, A., 2013. N-Alkane Evidence for the Onset of Wetter Conditions in the Sierra Nevada, California (USA) at the mid-late Holocene Transition, ~3.0 ka: Quaternary Research, vol. 79, pp. 14-23.

Thompson, G.R., 2014. Synchronous, millennial-scale climate changes between the northern Great Basin, USA, and Greenland in a time interval including the Mono Lake geomagnetic excursion. A thesis submitted to the Department of Geological Sciences, California State University, Bakersfield.

Tieszen, L.L., 1991. Natural variations in the carbon isotope values of plants: implications for archaeology, ecology, and paleoecology. Journal of Archaeological Science vol. 18, pp. 227–248.

Zic, M., Negrini, R.M., and Wigand, P.E., 2002. Evidence of Synchronous Climate Change across the Northern Hemisphere between the North Atlantic and the Northwestern Great Basin, United States: Geology, vol. 30, pp. 635-638.